

Figure 1. Low-energy conformer of sorbinil used as a template for definition of pharmacophoric points.

position of two or more molecules via their common pharmacophore points, (d) inspection of the composite molecule and intuitive design of the hybrid that tests the pharmacophoric hypothesis, (e) verification that a low-energy conformation of the hybrid can present the desired pharmacophore, and (f) elaboration of a synthetic pathway and synthesis of the hybrid molecule.

At the onset of this study, several basic assumptions were made. (1) It was assumed that sorbinil, tolrestat, and ICI-105,552 all act to inhibit aldose reductase by occupying the same site on the enzyme. If this assumption is true, then it should be possible to design a hybrid molecule that could contain features of tolrestat and one or more of the other orally active aldose reductase inhibitors. The assumption was an arbitrary one and one that could critically affect the results if it were false. However, in the absence of data to the contrary, it was used as a reasonable starting point. This same assumption has been used by others^{1b} in their design efforts. (2) The biologically relevant conformation of tolrestat was assumed to be that which matched the lowest energy conformation of sorbinil (see below) by superimposing a phenyl ring (concentric and coplanar) and an acidic proton. The requirement that two phenyl rings must be concentric and coplanar can be satisfied in two ways which essentially involve one ring being flipped by 180°. In the present study both of these possible overlaps were initially considered. However, one was selected visually only on the basis of better overlap between the other functional units contained in tolrestat and the molecule being superimposed. (3) The critical pharmacophoric requirement was assumed to be the exact spatial relationship between the acidic hydrogen and a phenyl group. This acidic hydrogen was chosen rather than the carboxylic oxygen to which it is bonded because it was quickly determined that tolrestat and ICI-105,552 placed the acidic hydrogen in the same position in space relative to the phenyl ring in rather different ways and that the expectation of overlap for the oxygens themselves was unreasonable (see Figure 5). (4) In ICI-105,552, the fused heterocyclic ring was assumed to be planar. Possible puckers of this ring that could seriously affect the outcome of this modeling were ignored.

Sorbinil, being the most rigid of the molecules to be compared, was treated first. Two conformational isomers were identified for sorbinil as low-energy conformations (i.e. within 3 kcal of one another by SYBYL SIMPLEX); these two conformers differed in the pucker of the non-benzenoid fused ring. Both conformers were initially considered, but the one that corresponded to the X-ray conformer was retained for further overlapping. This structure was minimized with MAXIMIN in SYBYL 3.4 (Tripose Associates, St. Louis, MO) and is shown in Figure 1 (Cartesian coordinates for all minimized structures are

available as supplementary material). The relative energies of this conformer and that of the minimized X-ray structure compared favorably at 5.118 and 5.188 kcal/mol, respectively.

The constrained grid search method that has been previously described⁶ was used to determine the "lowest" energy conformation for each molecule in question. Each of the rotatable bonds (i.e. exocyclic bonds in the molecule that were not restricted as double bonds or as amide bonds) was rotated about 360° in turn in steps of 10°. No other alteration was performed to the rest of the molecule and the resultant energy at each step was calculated. This results in an energy profile for rotation about the bonds studied. After profiles of this kind had been collected for all of the rotatable bonds in the given molecule, starting conformations for minimization were set up as all possible permutations and combinations of the torsional angle valley points of each rotatable bond. These starting conformations were then subjected to the SIMPLEX minimizer, and the lowest energy conformer found in this way was taken as the reference low-energy conformation.

The rotatable bonds were then moved freely in steps of 10° each (using the SYBYL SEARCH command) in an effort to find conformations that meet the given distance constraints of the pharmacophore. This methodology does not, for the moment, take account of energy in an explicit way, but only uses a van der Waals cutoff to determine allowed vs disallowed conformations. An energy investment of 3 kcal/mol or less in going from the "lowest" energy conformer to the one that meets the distance requirements of the pharmacophore was considered acceptable. This is based on the most conservative estimate of a hydrogen bond and on the assumption that binding will involve at least one such hydrogen bond. The energetics of allowed conformations were determined by minimizing them to completion with MAXIMIN. In addition, a check was performed after minimization to ensure that the process of minimization did not change the required distance constraints [points of the pharmacophore overlapped before and after minimization with an RMS fit of 0.15 (i.e. 10% of a C-C bond distance) or less].

The first molecule to be studied in this way was tolrestat. Two low-energy conformations of tolrestat were found that overlap well with the pharmacophoric requirements defined in the lowest energy conformer of sorbinil. These structures, A and B, differing in relative energies by 0.44 kcal/mol, are shown in Figure 2. Two ways were found to overlap tolrestat and sorbinil, each of them resulting

(6) (a) Humber, L.; Lee, D.; Treasurywala, A. *J. Mol. Graphics* 1985, 3, 84. (b) The Molecular Modeling work described in this paper was carried out by Dr. Adi Treasurywala and Deborah Loughney.

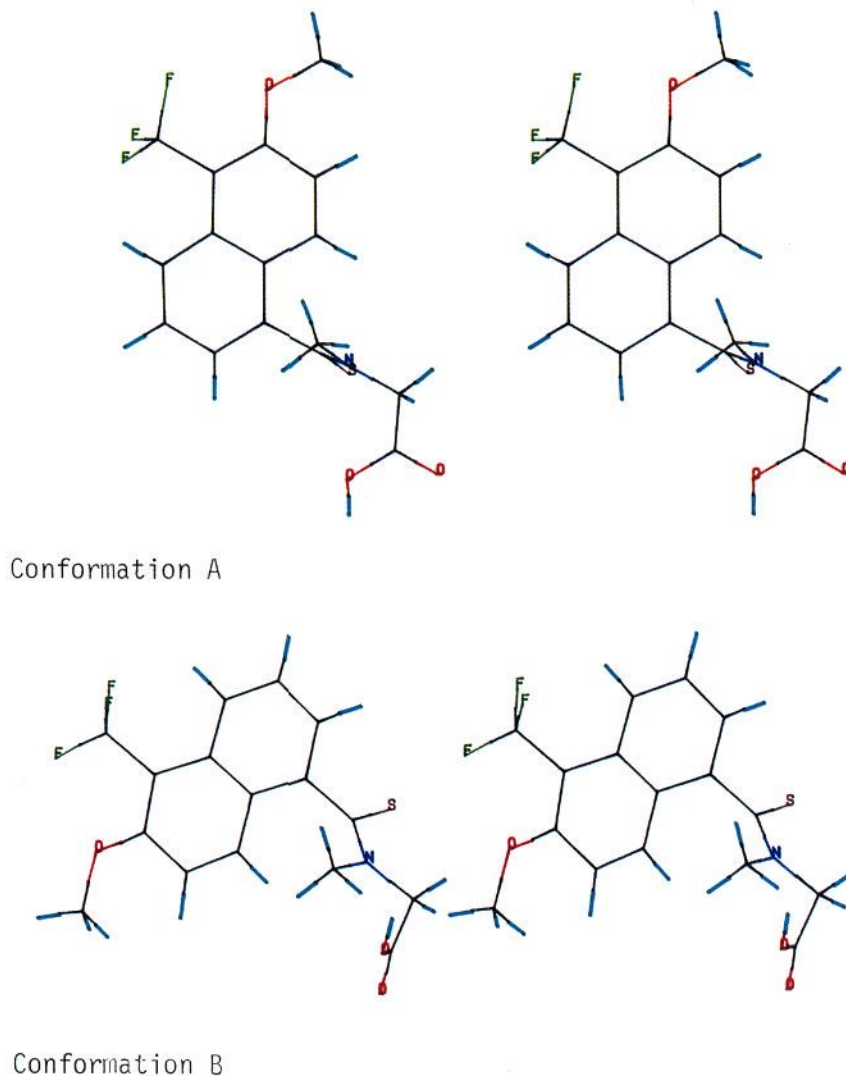


Figure 2. The low-energy conformations of tolrestat that match pharmacophoric requirements defined in the lowest energy conformer of sorbinil.

in a 180° flip of the ring system and a correspondingly different site chain conformation in tolrestat. The two compounds were superimposed with use of the FIT command in SYBYL. A centroid in the sorbinil phenyl ring and the thioamide-substituted phenyl ring of tolrestat was defined and the normal to the plane of the phenyl ring was determined, which extended 1 Å above and below that plane and intersected at the centroid. A fit was then performed with one end of the normal, the centroid, and the acidic proton. The resulting superimpositions and their RMS values are shown in Figure 3.

Thus, these studies showed that tolrestat and sorbinil can adopt low-energy conformations that present a common pharmacophore, namely a benzene ring whose centroid is 5.5–5.7 Å from an acidic proton that, in turn, is 0.8–1.2 Å above the plane of the phenyl ring. The two low-energy tolrestat conformations shown in Figure 2 defined the probable bioactive conformations of tolrestat that could be used as templates for the design of hybrids with other aldose reductase inhibitors such as, for example, ICI-105,552 (6). Both conformers of tolrestat appear to have acceptable overlap with sorbinil on the basis of energetics and RMS fit values. However, in the superimposition of conformer B (Figure 3b) there appeared to be little overlap between the molecules in areas other than

those which were specifically fitted together. For that reason, conformer A was selected for further modeling with ICI-105,552.

Low-energy conformations of ICI-105,552 were determined as described above by using the Constrained Grid Search to generate profiles for all rotatable bonds. Starting low-energy conformers were minimized using SIMPLEX. While using the SYBYL SEARCH command to find low-energy conformers that fit the distance constraints imposed by tolrestat conformer A, the flexible benzyl side chain of ICI-105,552 was set in a low-energy conformation as determined by the Constrained Grid Search involving rotation about both of the rotatable bonds in the benzyl group.

A low-energy conformation of ICI-105,552 that was minimized with MAXIMIN and meets the pharmacophoric requirements is shown in Figure 4. The structure is shown superimposed with the low-energy tolrestat conformation in Figure 5. The fit was performed as described above with the centroid of the aromatic rings, one end of the normals intersecting those centroids, and the acidic protons. An RMS value of 0.0559 was obtained for this fit. Initially, both the fused phenyl ring and the benzyl phenyl ring of ICI-105,552 were considered for overlap. However, a much poorer overlap was seen with the benzyl phenyl group; thus, it was not considered further. It is

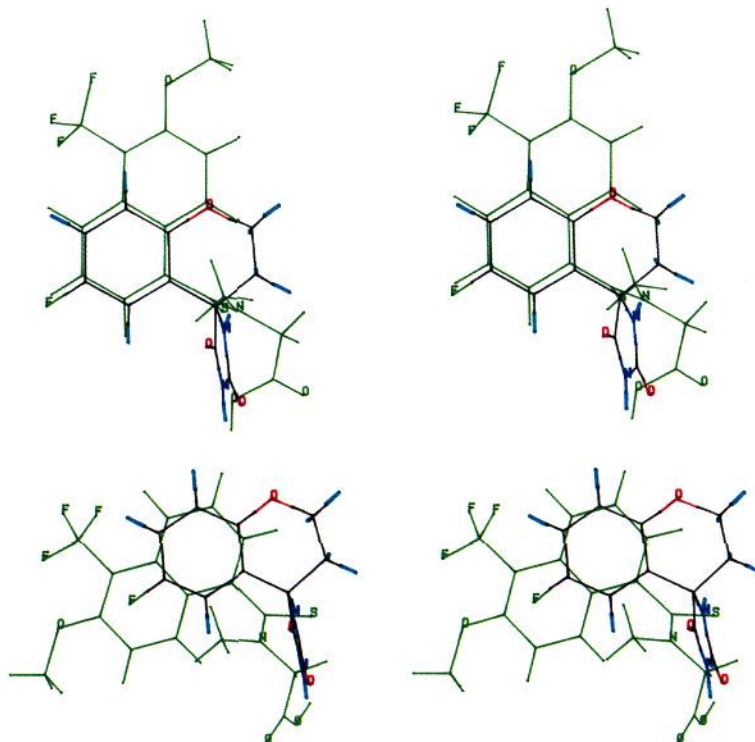


Figure 3. (Top, a) superimposition of tolrestat conformer A with sorbinil; RMS = 0.2462. (Bottom, b) superimposition of tolrestat conformer B with sorbinil; RMS = 0.1215.

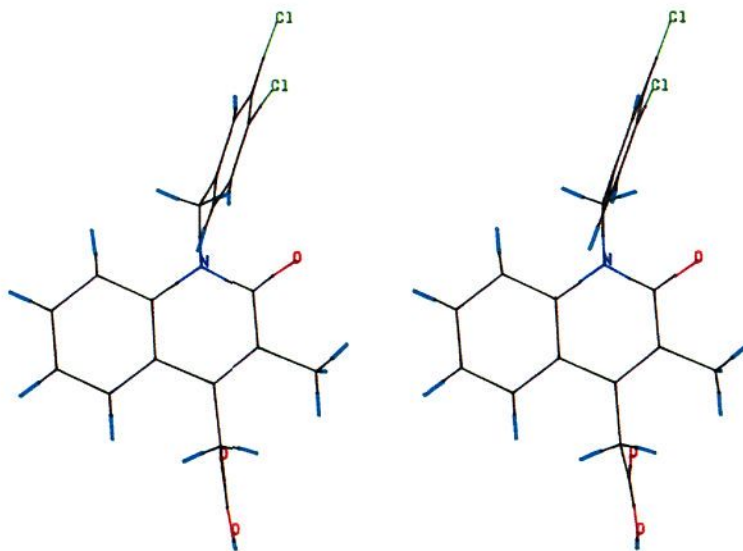


Figure 4. Low-energy conformation of ICI-105,552 that fits pharmacophoric constraints of tolrestat conformer A.

evident that the benzene ring of ICI-105,552 and that of tolrestat are almost coincident. An examination of where the noncoincident functionalities fell in these two molecules led to the design of 7-(trifluoromethyl)-8-methoxy-2-methyl-1-oxo-1*H*-phenalene-3-acetic acid (7) as a hybrid between tolrestat and ICI-105,552.

Low-energy conformations for hybrid compound 7 were generated as described above. A low-energy, minimized (MAXIMIN) conformation of 7 that contains the same pharmacophore that is believed to confer aldose reductase activity on tolrestat, sorbinil, and ICI-105,552 is shown in Figure 6a. The composite picture of hybrid 7, tolrestat, and ICI-105,552 shown in Figure 6b verifies that a low-

energy conformer of the hybrid can present the desired pharmacophore.

Chemistry

Our initial efforts toward the synthesis of phenalene 7 utilizing key tolrestat intermediate 8 is outlined in Scheme I. First, 6-methoxy-5-(trifluoromethyl)-1-naphthaldehyde (8)^{18a,24} was treated with carbon tetrabromide and triphenylphosphine in methylene chloride to give dibromomethylene compound 9, which was converted to propynoic ester 10 by treatment with *n*-butyllithium and methyl chloroformate. Triester 11 was obtained as a mixture of isomers (as shown by ¹H NMR) by treatment of 10 with

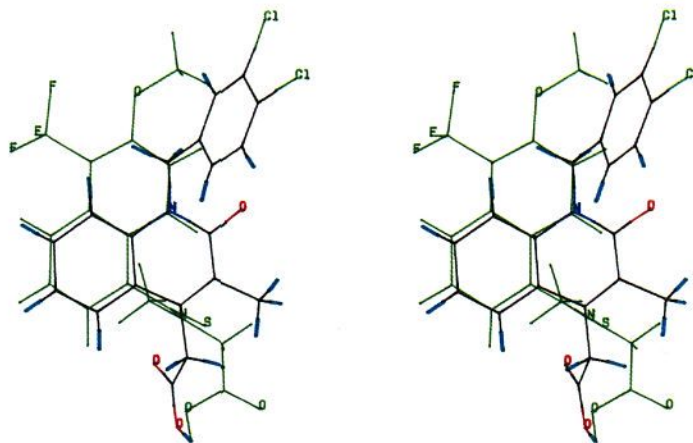
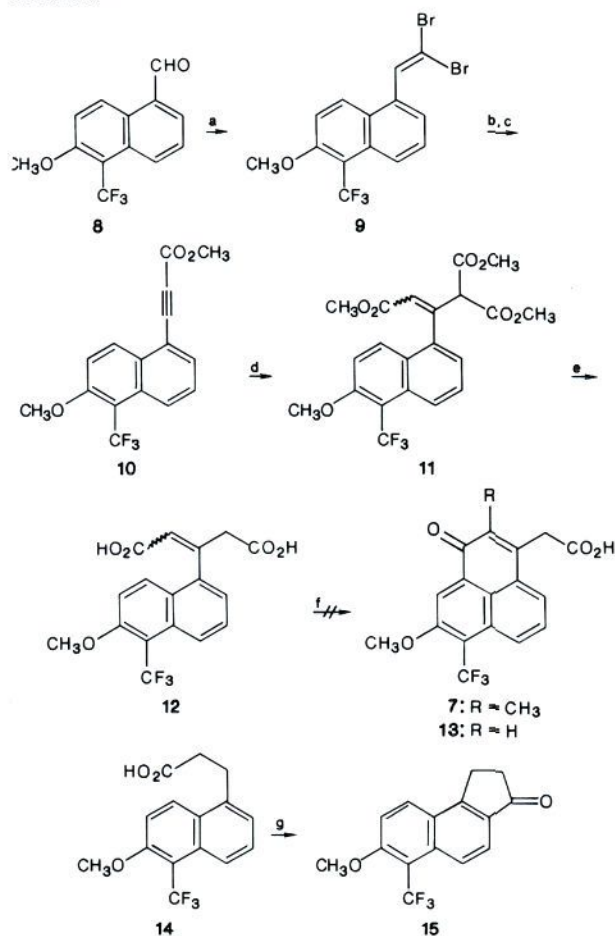


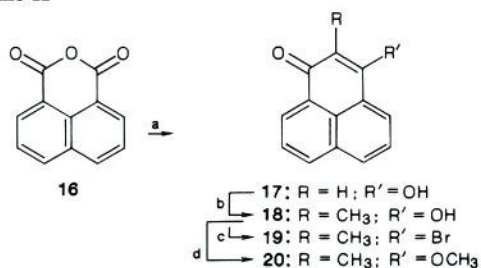
Figure 5. Superimposition of tolrestat with ICI-105,552; RMS = 0.0559.

Scheme I^a

the potassium salt of dimethyl malonate. Hydrolysis with concomitant decarboxylation afforded diacid 12. All attempts to obtain phenalene 13 from 12 via pericyclization (PPA,⁷ P_2O_5 , $\text{PCl}_5/\text{SnCl}_4$ ⁸) resulted in decomposition of starting material. The viability of this electronically un-

(7) Koo, J. *J. Am. Chem. Soc.* **1953**, *75*, 1891.

(8) Badger, G. M.; Carruthers, W.; Cook, J. W. *J. Chem. Soc.* **1949**, 1968.

Scheme II^a

favorable ring closure was tested by treatment of model acid 14 with polyphosphoric acid. This yielded cyclopentanone 15 as the only isolable organic product.²³ In light of these results, the above synthetic strategy was discontinued. In order to further study the synthetic feasibility, attention was directed toward the synthesis of unsubstituted analogue 26 as a model for hybrid 7.

Perinaphthindenedione 17, prepared according to the literature^{9,10} (Scheme II), was treated with methyl iodide and sodium ethoxide in a sealed vessel¹¹ to afford 18. Vinyl bromide 19 and enol ether 20 were prepared by bromination¹² and methylation, respectively, of dione 18 as shown. All attempts to introduce an acetic acid moiety onto 19 or 20 via nucleophilic displacement afforded instead 1,6-conjugate addition products.¹³

Stille and co-workers have reported the palladium(0)-catalyzed coupling of vinyl triflates with organostannanes.¹⁴ A more efficient synthesis of perinaphthindenedione 18, a precursor to triflate 24, is shown in Scheme III. 1-Naphthaldehyde was treated with the lithium anion of ethyl propionate to give alcohol 21, which was oxidized with Jones¹⁵ reagent to afford β -keto ester 22. Cyclization

(9) Errera, G. *Gazz. Chim. Ital.* **1911**, *41*, 190.

(10) Eistat, B.; Ganster, O. *Liebigs Ann. Chem.* **1969**, *723*, 188.

(11) Geissman, T. A.; Morris, L. *J. Am. Chem. Soc.* **1944**, *66*, 716.

(12) Piers, E.; Grierson, J. R.; Lau, C. K.; Nagakura, I. *Can. J. Chem.* **1982**, *60*, 210.

(13) This type of reactivity of perinaphthindenediones has been reported: Kowlsch, C. F.; Rosenwald, R. H. *J. Am. Chem. Soc.* **1937**, *59*, 2166.

(14) Scott, W. J.; Crisp, G. T.; Stille, J. K. *J. Am. Chem. Soc.* **1984**, *106*, 4630.

(15) Bodwen, K.; Heilbron, I. M.; Jones, E. R. H.; Weedon, B. C. L. *J. Chem. Soc.* **1946**, 39.

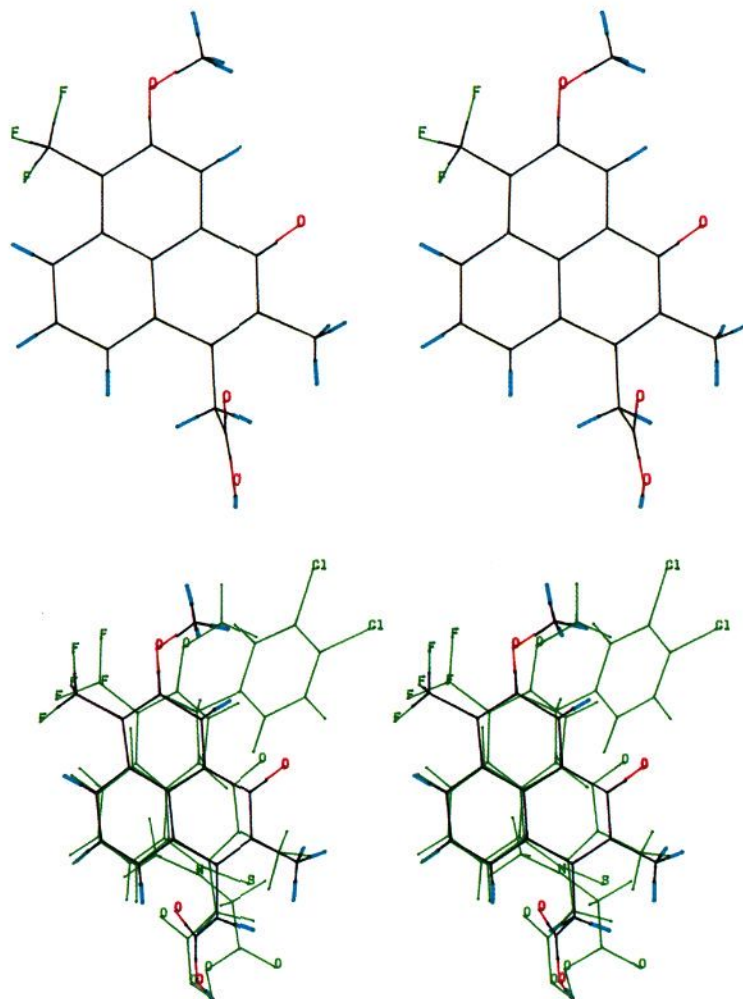


Figure 6. (Top, a) low-energy conformer of hybrid 7. (Bottom, b) superimposition of hybrid 7 with tolrestat and ICI-105,552.

with concentrated sulfuric acid¹⁶ afforded an easily separable mixture (1:1) of 2-methylperinaphthindenedione 18 and 2-methyl-4,5-benzoinindandione 23. Treatment of 18 with triflic anhydride/pyridine afforded vinyl triflate 24, which was converted to the 3-allyl derivative 25 with allyltributyltin, palladium tetrakis(triphenylphosphine) and lithium chloride.¹⁴ Unmasking the carboxymethyl moiety was easily accomplished by treatment with osmium tetroxide and sodium periodate¹⁷ followed by Jones reagent to afford phenalene derivative 26 (AY-31,358) as a highly colored yellow solid. AY-31,358 was evaluated as an aldose reductase inhibitor.

Results and Discussion

Hybrid analogue 26 (AY-31,358) was tested in vitro as an inhibitor of partially purified bovine lens aldose reductase¹⁸ and in the in vitro rat sciatic nerve assay.¹⁹ The

Table I. Aldose Reductase Inhibition in Vitro by 26, 27, and Tolrestat (1)

compd	IC ₅₀ , ^a M	
	bovine lens aldose reductase	isolated rat sciatic nerve
26	2.4 × 10 ⁻⁷	2.5 × 10 ⁻⁶
27	7.3 × 10 ⁻⁷	inactive ^b
1	3.5 × 10 ⁻⁸	5.4 × 10 ⁻⁷

^a Concentration required to produce 50% inhibition of enzymatic activity or polyol accumulation. ^b <15% inhibition at 1 × 10⁻⁵ M.

Table II. Inhibition of Galactitol Accumulation in the Lens and Sciatic Nerve of Rats Fed 20% Galactose Chow for 4 Days

compd	dose, mg/kg	inhibn of galactitol accumulation, %	
		lens	sciatic nerve
26	76	NS ^a	35
27	159	NS	NS
1	26	15	94

^a Galactitol levels in the drug-treated animals were not significantly different from that in the galactosemic control animals (*p* > 0.05).

compound was also screened in vivo by using the 4-day galactosemic rat model²⁰ in which rats were kept on a 20%

(16) Wojack, G. *Chem. Ber.* 1938, 71, 1102.

(17) Pappo, R.; Allen, D. S.; Lemieux, R. U.; Johnson, W. S. *J. Org. Chem.* 1956, 21, 478.

(18) (a) Sestanj, K.; Bellini, F.; Fung, S.; Abraham, N.; Treasurywala, A.; Humber, L.; Simard-Duquesne, N.; Dvornik, D. *J. Med. Chem.* 1984, 27, 255. (b) Hayman, S.; Kinoshita, J. H. *J. Biol. Chem.* 1965, 240, 877.

(19) (a) Sredy, J.; Millen, J.; McCaleb, M. L.; Tutwilier, G. F. *Fed. Proc., Fed. Am. Soc. Exp. Biol.* 1986, 45, 902. (b) Bergmeyer, Y.; Guber, W.; Gutman, I. D-Sorbitol. In *Methods of Enzymatic Analysis*; Bergmeyer, H. V., Ed.; Academic Press Inc.: New York, 1974; Vol. 3.

(20) (a) Simard-Duquesne, N.; Greselin, E.; Dubuc, J.; Dvornik, D. *Metabolism* 1985, 34, 885. (b) Kraml, M.; Cosyns, L. *Clin. Biochem.* 1969, 2, 373.

